NANO LETTERS

2007
Vol. 7, No. 12
3792−3797

Vacuum-Breakdown-Induced Needle-Shaped Ends of Multiwalled Carbon Nanotube Yarns and Their Field Emission Applications

Yang Wei,* Kaili Jiang, Liang Liu,* Zhuo Chen, and Shoushan Fan

Tsinghua-Foxconn Nanotechnology Research Center, Tsinghua University, Beijing 100084, People's Republic of China

Received September 9, 2007; Revised Manuscript Received October 15, 2007

ABSTRACT

The Joule-heating-induced vacuum breakdown of the carbon nanotube (CNT) yarns was studied. Wall-by-wall breakdown and superplastic deformation of CNTs are the main physical processes at the hottest location before breakdown. The two ends at the breaking point are needle-shaped with surfaces rich in tightly compacted conelike CNT bundles with a single CNT at the tips. Both of the ends can provide emission currents of over 150 μA within an area 5 μm in diameter; the cathode ends start field emission at a lower voltage. Laser irradiation was introduced to control the breaking location making the methodology more practical. Small pixels were constructed with the yarn emitter cathodes, which are potentially building blocks of large outdoor displays.

Carbon nanotubes (CNTs) are promising 1D nanomaterials, thanks to their high aspect ratio, high electrical and thermal conductivity, great mechanical strength, and chemical inertness.[1,2] CNT arrays are self-assembled structures, where CNTs of high quality are vertically aligned on substrates.[3−6] Super-aligned multiwalled CNT (MWNT) arrays were first synthesized by our group in 2002.[7] The CNTs in such arrays have very clean surfaces and strong van der Waals interaction with neighboring CNTs, and the strong intertube interactions allow continuous MWNT thin sheets to be directly dry spun from them.[8] After passing through volatile solvents, the MWNT sheets will shrink to a tight yarn like a fiber where the MWNTs are close packed leading to a high tensile strength.[9] The macroscopic configuration makes the nanotubes easy to manipulate.

Besides the incandescent lamp applications proven in 2002, we have recently developed two novel electronics-oriented applications for these yarns. One is as thermionic emission electron sources based on high temperature;[10,11] the other is as cold cathodes with the mechanically cut cross section as the effective field emitters.[12] Some basic problems need to be clarified in these practical applications. The behaviors especially the vacuum breakdown at high temperature induced by Joule heating should be studied, since it decides the work ceiling in high-temperature dependent applications such as hot filament and thermionic emission. The cross section of a MWNT yarn can provide a milliampere-level emission current. However, because of the mechanical contact, the mechanically cut surface is usually covered with some organic remnants that are difficult to remove and detrimental for field emission. Furthermore, the controllability of the mechanical cutting is still low. So it is necessary to develop a noncontacting method to improve the controllability and surface cleanness. It is a possible solution to fabricate a high-quality field electron emitter from MWNT yarns by the vacuum breakdown process.

In this letter, we studied the vacuum breakdown process caused by Joule heating, investigated the field emission behaviors of the two ends at the breaking point, and have made some interesting discoveries. The two ends were composed of conelike CNT bundles having a single CNT at the tip. The diameter of CNTs at the tips was about 5 nm, which is much less than the as-grown super-aligned MWNTs. The shrinking of CNTs at the breaking point is attributed to the CNT's superplastic deformation.[14] Field emission tests on these ends showed that they can provide emission currents of over 150 μA with a calculated current density of over 700 A/cm^2. The breaking location was successfully controlled by introducing local defects with laser irradiation in air, which makes the vacuum breakdown methodology more valuable. To test an application, we constructed a new type of small pixel with the yarn emitter cathode. The self-assembled tips could have many other potential applications.

A 2 cm long MWNT yarn with a diameter of 25 μm was suspended between two 0.5 mm diameter copper wires. A 40 V DC bias was applied to heat the yarn under a vacuum

* Corresponding authors. E-mail: (Y.W.) weiy02@mails.tsinghua.edu.cn; (L.L.) liuliang@mail.tsinghua.edu.cn.

10.1021/nl072298y CCC: $37.00
Published on Web 11/16/2007

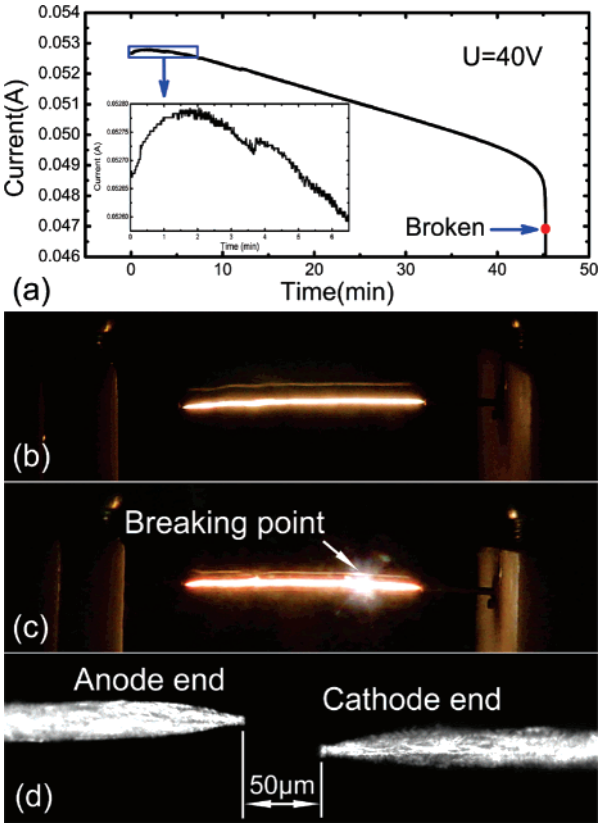

Figure 1. (a) Vacuum breakdown process of the hot CNT yarns induced by Joule heating monitored by a Keithley 237 sourcemeter. (b) A uniform incandescent MWNT yarn. (c) The hottest spot appears that will then become the breaking point. (d) An optical micrograph of the breaking point showing both ends are needle-shaped and have a 50 μm gap between them.

of 2×10^{-5} Pa. Figure 1b shows the uniform incandescent MWNT yarn. The temperature was determined by fitting the incandescent light spectrum with the blackbody radiation law;[11,12] it was approximately 2213 K at the start of the experiment. The time dependent current was monitored by a Keithley 237 sourcemeter, which is shown in Figure 1a. The resistance was first reduced and terminated fast (inset of Figure 1a). Then the resistance increased slowly until the hottest spot appeared (Figure 1c). The current decreased exponentially, and the CNT yarn was broken at the hottest point. The whole process took less than 1 h. In 2002, we reported that the conductivity of the yarn continuously increased during the 3 h DC vacuum annealing.[7] In 2006, we annealed the MWNT yarn at 1881 K for about 5 h under vacuum to improve the mechanical strength without vacuum breakdown.[12] Both the fast-terminated resistance reduction process and the vacuum breakdown can thus be attributed to the higher temperature adopted here, which was over 2200 K.

An optical microscope observation on the breaking point is shown in Figure 1d. The two ends (anode end and cathode end) look like needles but not very sharp, and the gap between them is about 50 μm. They are not positively aligned but have a mismatch. The needle-shaped ends should be intuitively attributed to the carbon sublimation or evaporation induced by the local high temperature, which should be much higher than 2200 K.

CNTs are seamless tubules with a carbon honeycomb net. It is necessary to clarify what remained at the breaking point after some of the carbon was removed from such seamless tubes by evaporation or sublimation. SEM observations were performed on both ends. Figure 2a is the full view of the anode end; Figure 2b is the cathode end. Higher magnification images of them are shown in Figure 2c,d, respectively. The ends are about 5 μm in diameter and are composed of tiny conelike tips. The difference between them is that the tip number at the cathode end is much more than the anode end. The tips at the cathode end have larger aspect ratios. The asymmetric morphologies might be caused by the high local electric field and low vacuum at moment of breakdown instant. Discharge might happen between the gap at that moment and the ion bombardment splits the big tips (Figure 2c) into many small tips. Surprisingly, SEM observation did not reveal any CNTs at the end tips, although the yarn consists of CNTs and the morphology does not have apparent change besides the end zone.

The tips were further studied by TEM. They are conical CNT bundles as shown in Figure 3. Figure 3a,b are the tips at the anode end; Figure 3c,d are the tips at the cathode end. They are generally composed of well-aligned and firmly compacted CNTs with a single CNT at the tip. The CNTs at the tip are about 5 nm in diameter and customarily have 2 or 3 walls. The diameter of the as-grown CNTs is about 15 nm, and they have more than 5 walls.[9] It can thus be concluded that both the CNT diameter and the number of the graphite layers were decreased by the vacuum breakdown process. These agree with experiments of Ren's group. They validated Joule-heating-induced wall-by-wall breakdown of MWNTs at temperatures higher than 2000 °C,[13] and they observed current decrease during the wall-by-wall breakdown process. They also reported the superplastic deformation of CNTs induced by high temperatures and kinks.[14−16] Hot CNTs can be elongated under a tensile load, leading to a reduction in diameter. On the basis of these results, both the reduction of the conductivity and the decrease in the number of walls should be attributed to the wall-by-wall breakdown of the CNTs at the hottest spot where the temperature is higher than 2200 K. The shrunk diameter and well-aligned structure are due to superplastic elongation by tensile loading. The tensile stress in the suspended MWNT yarn could be inferred from the mismatch and gap between the separated two ends after breaking (Figure 1d). The CNTs at the tips are compacted tightly. This may be caused by the capillary force induced by the melted carbon at the breakdown instant. The capillary force shrinks the CNTs together tightly.

The formation of such special morphology is therefore the result of the high temperature, tensile loading, instant melting, and high local electric field at the breaking point.

Some groups have proven that high-temperature annealing can efficiently remove the defects in CNTs, consequently improving electric and thermal conductivity, and mechanical strength.[18−21] Figure 4 shows the Raman spectra of the MWNT yarn before and after vacuum annealing (blue and

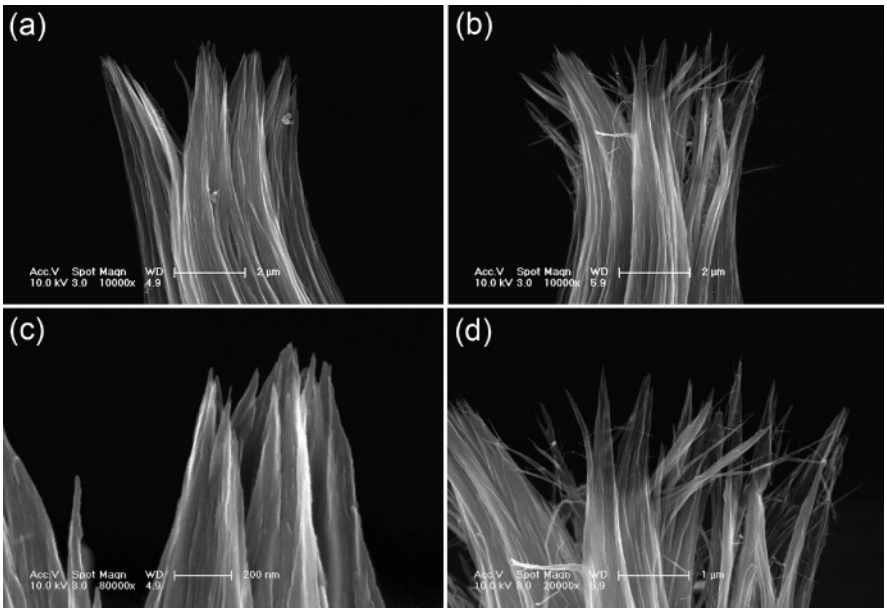

Figure 2. (a) SEM image of the anode end at breaking point. Scale bar: 2 μm. (b) SEM image of the cathode end at breaking point. Scale bar: 2 μm. (c) Higher magnification image of one big tip at the anode end; this image shows that the big tip at the anode end is composed of some small tips. Scale bar: 200 nm. (d) Higher magnification image of the tips at the cathode end. Scale bar: 1 μm.

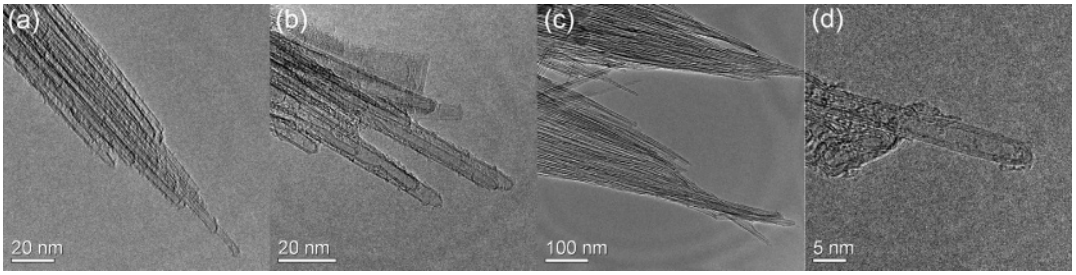

Figure 3. TEM image of the conelike tips at the breaking point of CNT yarns. (a) and (b) are the anode end; (c) and (d) are the cathode end.

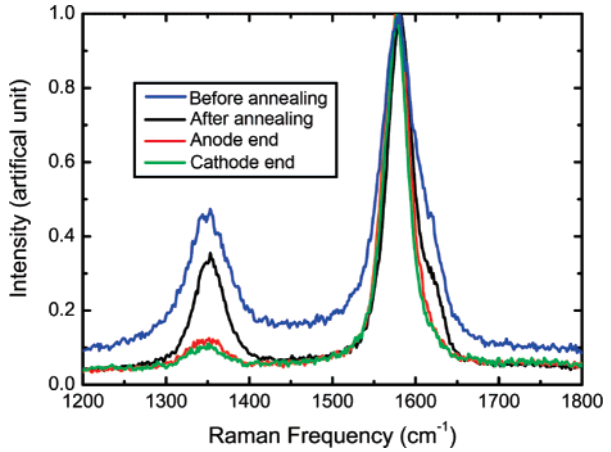

Figure 4. Raman spectra of the as-fabricated MWNT yarn before and after vacuum annealing (blue and black solid lines) and the Raman spectra of the anode and cathode ends at the breaking point (red and green solid lines).

black solid lines) and Raman spectra of the ends at the breaking point (red and green solid lines). Effective removal of the structural defects by high-temperature annealing is strongly supported by the low-intensity D-band (defect mode) at 1350 cm^{-1}. Most striking is that the end tips have the best quality, despite most of their body having expired into the vacuum.[14] Ding et al. have suggested that the pentagon−heptagon cores make the evaporating CNTs retain their perfection.[17] The high quality may also in part be due to the defect-abundant layers being removed by wall-by-wall breakdown[13] and the remaining amorphous carbon being evaporated efficiently by the high temperature at the instant of breakdown.

The vacuum breakdown induces the formation of conical CNT bundles made up of high-quality CNTs with a single CNT, 5 nm in diameter, at the tip. The CNT tips nearest the end are firmly held by the lower CNTs. The mechanical and electrical contact of the uppermost CNT tips should be very good. The improved-quality CNTs have better electrical and thermal conductivity. All these tell us that these ends should be good field emitters with small cross sections (5 μm in diameter at the ends).

Both the anode and cathode ends were fixed using silver paste to copper wires, 0.5 mm in diameter, along their axis direction. The length of the yarn emitters was 3 mm. The yarn emitters were assembled in a custom-made testing apparatus that included a three-dimensional (3D) manipulator. The yarn emitter was fixed to a holder and a tungsten

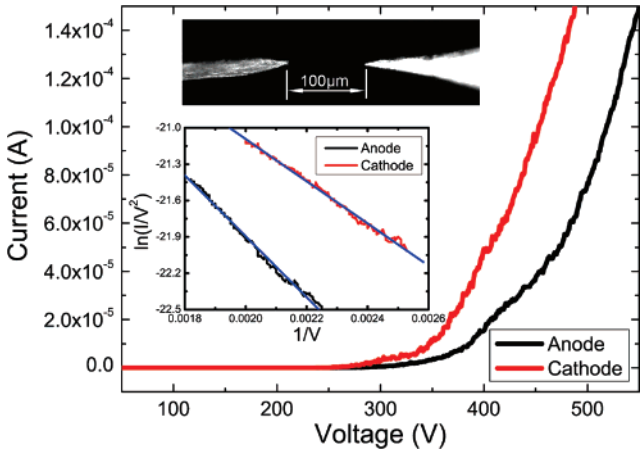

Figure 5. Field emission properties of the anode and cathode ends fabricated by vacuum breakdown process. Both can provide emission currents of over 150 μA. The top inset shows the testing method using a tungsten probe as anode with a 100 μm gap. The bottom inset is the FN curves.

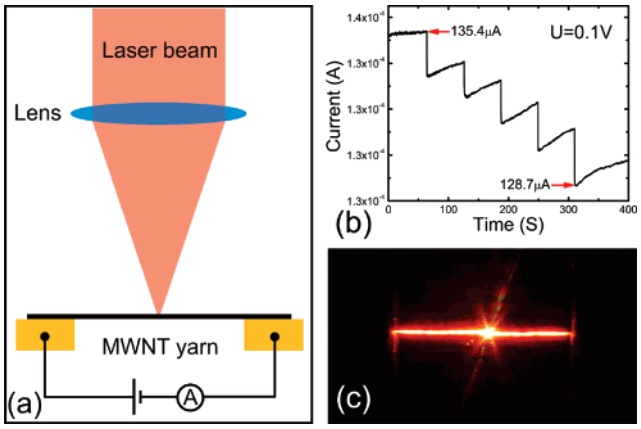

Figure 6. (a) Schematic illustration of the laser irradiation in air to introduce defects into MWNT yarns. (b) Abrupt current drops induced by laser irradiation. (c) The laser irradiation location becomes the hottest spot and will be the breaking point.

probe was fixed to the 3D manipulator as the anode. With the 3D manipulator, the yarn emitter and the tungsten probe were oppositely aligned with a 100 μm gap (the top inset of Figure 5). The emission current was monitored as a function of the applied voltage using a Keithley 2410 sourcemeter under a vacuum of 2×10^{-5} Pa.

Figure 5 shows the typical IV curves of the as-fabricated yarn emitters. The threshold voltage of electron emission is about 300 and 250 V for the anode and cathode end, respectively. Both of them could provide emission currents of over 150 μA. The current density can be calculated as being over 700 A/cm^2. The corresponding Fowler−Nordheim (FN) plot ($\ln I/V^2 \sim 1/V$) is shown in the bottom inset of Figure 5; the straight line indicates pristine field emission from the clean CNT emitters. The work function of CNT was taken as 4.6 eV,[10] and field enhancement factors from the slopes of FN plot were 2677 for anode end and 3873 for cathode end.

The most impressive feature of this type of yarn emitter is that it can provide large currents (over 150 μA) within a very small area (5 μm in diameter). The current density (700 A/cm^2) is much higher than the yarn emitter fabricated by mechanical cutting (200 A/cm^2).[12] The mechanically cut cross sections of the MWNT yarn have dense effective emission sites ensuring the large emission current density. The needle-shaped ends fabricated by vacuum breakdown only have a few conical CNT bundles that perform field emission; however, these can provide even larger emission current density. An individual cone tip thus carries a much larger emission current. Failure of field-emitting CNTs is usually caused by the Joule heating from the emission current[22−24] or the electric force on the CNT tips.[25] The single CNT at the cone tip is very short and firmly caught by neighboring CNTs, and these tubes' quality are greatly improved by high-temperature annealing. The field-emitting CNT at the tip can thus withstand a large electric force because of its tight mechanical contact, and the Joule heat can be efficiently conducted as the CNTs at the tips are short and well connected to the neighboring CNTs. Moreover, the field emission capability of such an individual conical tip is worthy of expectation. We are pursuing further experiments to characterize its field emission capability as point electron sources.[26−28]

Two main factors contribute to the field enhancement factor: the shrunk CNTs with smaller diameter induced by superplastic elongation[29,30] and the separation of individual tips, which effectively decreases the screening effect between the neighboring emission sites.[31] The tips at the cathode end have higher aspect ratio deciding its larger enhancement factor.

Field emission tests showed that both of the two ends at the breaking point are excellent field emitters. They can thus potentially be used as the cold cathodes in the vacuum electronic devices. But the location of the breaking point could not be precisely controlled, hindering their practical application. Here, we introduced defects on a local position of the MWNT yarns by laser irradiation and successfully controlled the breaking location. The process is schematically illustrated in Figure 6a. A focused CO_2 laser beam scanned along perpendicular bisector of the suspended MWNT yarn in air. The laser power was 12 W and the scanning velocity was 1000 mm/S. By applying a 0.1 V bias on the MWNT yarn, we can see an abrupt current drop at the instant of laser burning (Figure 6b). It was repeated 5 times. The conductivity was reduced by about 5%. Power consumption of Joule heating is proportional to the resistance in series circuit, so the defect-abundant midpoint will be the hottest spot (Figure 6c) and final breaking point. The laser burning method enables the vacuum breakdown technology to be used to efficiently fabricate the MWNT yarn field emitters.

The as-fabricated yarn emitters are high-yield and low-cost. A super-aligned CNT array on one 4 in. wafer can produce CNT yarns over 100 m long, while the length of the yarn emitters is less than 1 cm. Thus, the MWNT array grown on one 4 in. wafer could produce thousands of such emitters. The wafer can be used again, which is environmentally friendly and can lower the cost effectively. The

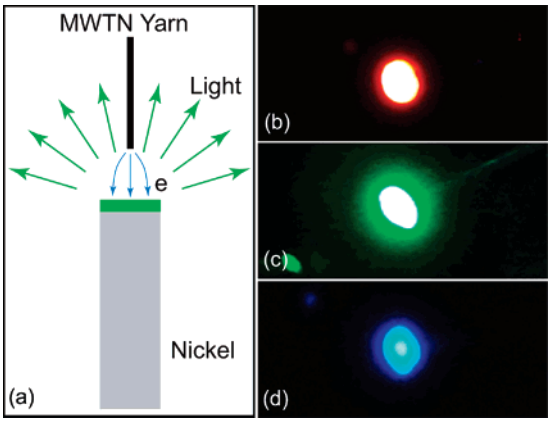

Figure 7. (a) Schematic illustration of the structure of the small pixel with a MWNT yarn as the cathode and phosphor-coated cross section of a nickel rod as the anode. Panels b−d are RGB pixels tested in dynamic vacuum.

vacuum process and laser irradiation are all low-cost industrialized processes.

To show the probable application in vacuum electronic devices, we assembled the yarn emitter into a new type of pixels as cold cathodes and tested them under dynamic vacuum. The structure of the pixel is illustrated in Figure 7a. The cross section of a nickel rod with a diameter of 1 mm was first polished and then coated with a layer of phosphor. The MWNT yarn emitter was pointed at the center of phosphor-coated surface with a 0.5 mm gap. When a positive voltage was applied on the nickel, the end of the MWNT yarn would emit electrons exciting the phosphor to emit light. The polished cross section reflects light back, which is similar to the Al film in the conventional cathode ray tubes (CRTs). This might improve the brightness. The metallic anode efficiently conducts the heat induced by the electron bombardment. The cool anode will improve the lifetime of future sealed devices. Figure 7b−d are the lit red, green, and blue (RGB) pixels. The voltage applied on the anode was 650 V, and the emission current was about 100 μA.

Some progress has been achieved by others and us on applying CNTs as the cathodes of luminescent tubes and the cathodes of field emission displays.[32−36] The cathode ray tube lighting elements[32,33] can be possibly used to construct displays, but their applications as large outdoor displays with high resolution are currently being limited by the large diameters of the luminescent zone, which are about 20 mm. The pixels suggested here have much smaller diameter and may enable progress in this area. The pixel might also find applications as portable light sources.

One could imagine that the yarn emitters can be integrated into some other devices such as electron guns, X-ray tubes,[37] saddle gauges,[38] and etc. Besides the field emission application, the individual conelike bundles with a single CNT at the tip can be potentially used as probes of atomic force microscopy and scanning tunneling microscopy.[39] The vacuum breakdown methodology will become more valuable if it can fabricate a conical tip with a single-walled CNT nearest the end. It will be possible by controlling the tensile loading and the breakdown process.

In summary, we studied the Joule-heating vacuum breakdown process of CNT yarns. Both the anode end and cathode end at the breaking-point are needle-shaped like a tungsten probe. The ends are rich in tightly compacted tiny CNT bundles with a single CNT at the tips. The diameter of CNTs at the tips is about 5 nm: much less than the as-grown super aligned MWNTs. This has been attributed to the CNTs' superplastic deformation. Field emission tests show that they can provide over 150 μA emission currents within very small areas, such as 5 μm in diameter. Laser irradiation was suggested to control the location of the breaking point. On the basis of these studies, a new type of small pixel was constructed with the yarn emitter as the cathode. The small pixels are potential building blocks for large outdoor displays. The self-assembled tips should have many other potential applications, such as electron sources for X-ray tubes, point electron sources, probes of scanning probe microscopy and so on.

Acknowledgment. The authors thank Sam Roots for proofreading. We gratefully acknowledge the financial support from National Basic Research Program of China (2005CB623606) and NSFC (10334060).

References

(1) Iijima, S. *Nature* **1991**, *354*, 56.
(2) Saito, R.; Dresselhaus, G.; Dresselhaus, M. S. *Physical Properties of Carbon Nanotubes*; World Scientific Publishing Company: Singapore, 1998.
(3) Li, W. Z.; Xie, S. S.; Qian, L. X.; Chang, B. H.; Zou, B. S.; Zhou, W. Y.; Zhao, R. A.; Wang, G. *Science* **1996**, *274*, 1701.
(4) Ren, Z. F.; Huang, Z. P.; Xu, J. W.; Wang, J. H.; Bush, P.; Siegal, M. P.; Provencio, P. N. *Science* **1998**, *282*, 1105.
(5) Fan, S. S.; Chapline, M. G.; Franklin, N. R.; Tombler, T. W.; Cassell, A. M.; Dai, H. J. *Science* **1999**, *283*, 512.
(6) Hata, K.; Futaba, D. N.; Mizuno, K.; Namai, T.; Yumura, M.; Iijima, S. *Science* **2004**, *306*, 1362.
(7) Jiang, K. L.; Li, Q. Q.; Fan, S. S. *Nature* **2002**, *419*, 801.
(8) Zhang, M.; Fang, S. L.; Zakhidov, A. A.; Lee, S. B.; Aliev, A. E.; Williams, C. D.; Atkinson, K. R.; Baughman, R. H. *Science* **2005**, *309*, 1215.
(9) Zhang, X. B.; Jiang, K. L.; Feng, C.; Liu, P.; Zhang, L.; Kong, J.; Zhang, T. H.; Li, Q. Q.; Fan, S. S. *Adv. Mater.* **2006**, *18*, 1505.
(10) Liu, P.; Wei, Y.; Jiang, K. L.; Sun, Q.; Zhang, X. B.; Fan, S. S.; Zhang, S. F.; Ning, C. G.; Deng, J. K. *Phys. Rev. B* **2006**, *73*, 235412.
(11) Wei, Y.; Jiang, K. L.; Feng, X. F.; Liu, P.; Liu, L.; Fan, S. S. *Phys. Rev. B* **2007**, *76*, 045423.
(12) Wei, Y.; Weng, D.; Yang, Y. C.; Zhang, X. B.; Jiang, K. L.; Liu, L.; Fan, S. S. *Appl. Phys. Lett.* **2006**, 89, 063101.
(13) Huang, J. Y.; Chen, S.; Jo, S. H.; Wang, Z.; Han, D. X.; Chen, G.; Dresselhaus, M. S.; Ren, Z. F. *Phys. Rev. Lett.* **2005**, *94*, 236802.
(14) Huang, J. Y.; Chen, S.; Wang, Z. Q.; Kempa, K.; Wang, Y. M.; Jo, S. H.; Chen, G.; Dresselhaus, M. S.; Ren, Z. F. *Nature* **2006**, *439*, 281.
(15) Huang, J. Y.; Chen, S.; Ren, Z. F.; Wang, Z. Q.; Wang, D. Z.; Vaziri, M.; Suo, Z.; Chen, G.; Dresselhaus, M. S. *Phys. Rev. Lett.* **2006**, *97*, 075501.
(16) Huang, J. Y.; Chen, S.; Ren, Z. F.; Wang, Z.; Kempa, K.; Naughton, M. J.; Chen, G.; Dresselhaus, M. S. *Phys. Rev. Lett.* **2007**, *98*, 185501.
(17) Ding, F.; Jiao, K.; Lin, Y.; Yakobson, B. I. *Nano Lett.* **2007**, *7*, 681.
(18) Kim, Y. A.; Hayashi, T.; Osawa, K.; Dresselhaus, M. S.; Endo, M. *Chem. Phys. Lett.* **2003**, *380*, 319.
(19) Jin, R.; Zhou, Z. X.; Mandrus, D.; Ivanov, I. N.; Eres, G.; Howe, J. Y.; Puretzky, A. A.; Geohegan, D. B. *Physica B* **2007**, *388*, 326.
(20) Gong, Q. M.; Li, Z.; Wang, Y.; Wu, B.; Zhang, Z.; Liang, J. *Mater. Res. Bull.* **2007**, *42*, 474.
(21) Chen, J.; Shan, J. Y.; Tsukada, T.; Munekane, F.; Kuno, A.; Matsuo, M.; Hayashi, T.; Kim, Y. A.; Endo, M. *Carbon* **2007**, *45*, 274.

(22) Huang, N. Y.; She, J. C.; Chen, J.; Deng, S. Z.; Xu, N. S.; Bishop, H.; Huq, S. E.; Wang, L.; Zhong, D. Y.; Wang, E. G.; Chen, D. M. *Phys. Rev. Lett.* **2004**, *93*, 075501.
(23) Liang, X. H.; Deng, S. Z.; Xu, N. S.; Chen, J.; Huang, N. Y.; She, J. C. *Appl. Phys. Lett.* **2006**, *88*, 111501.
(24) Wei, W.; Liu, Y.; Wei, Y.; Jiang, K. L.; Peng, L. M.; Fan, S. S. *Nano Lett.* **2007**, *7*, 64.
(25) Wei, W.; Jiang, K. L.; Wei, Y.; Liu, M.; Yang, H. T.; Zhang, L. N.; Li, Q. Q.; Liu, L.; Fan, S. S. *Nanotechnology* **2006**, *17*, 1994.
(26) Fransen, M. J.; van Rooy, T. L.; Kruit, P. *Appl. Surf. Sci.* **1999**, *146*, 312.
(27) de Jonge, N.; van Druten, N. J. *Ultramicroscopy* **2003**, *95*, 85.
(28) de Jonge, N.; Lamy, Y.; Schoots, K.; Oosterkamp, T. H. *Nature* **2002**, *420*, 393.
(29) Bonard, J. M.; Dean, K. A.; Coll, B. F.; Klinke, C. *Phys. Rev. Lett.* **2002**, *89*, 197602.
(30) Edgcombe, C. J.; Valdre, U. *Philos. Mag. B* **2002**, *82*, 987.
(31) Nilsson, L.; Groening, O.; Emmenegger, C.; Kuettel, O.; Schaller, E.; Schlapbach, L.; Kind, H.; Bonard, J. M.; Kern, K. *Appl. Phys. Lett.* **2000**, *76*, 2071.
(32) Saito, Y.; Uemura, S.; Hamaguchi, K. *Jpn J. Appl. Phys.* **1998**, *37*, L346−L348.
(33) Saito, Y.; Uemura, S. *Carbon* **2000**, *38*, 169.
(34) Bonard, J. M.; Stöckli, T.; Noury, O.; Châtelain, A. *Appl. Phys. Lett.* **2001**, *78*, 2775.
(35) Wei, Y.; Xiao, L.; Zhu, F.; Liu, L.; Tang, J.; Liu, P.; Fan, S. S. *Nanotechnology* **2007**, *18*, 325702.
(36) Choi, W. B.; Chung, D. S.; Kang, J. H.; Kim, H. Y.; Jin, Y. W.; Han, I. T.; Lee, Y. H.; Jung, J. E.; Lee, N. S.; Park, G. S.; Kim, J. M. *Appl. Phys. Lett.* **1999**, *75*, 3129.
(37) Sugie, H.; Tanemura, M.; Filip, V.; Iwata, K.; Takahashi, K.; Okuyama, F. *Appl. Phys. Lett.* **2001**, *78*, 2578.
(38) Sheng, L. M.; Liu, P.; Wei, Y.; Liu, L.; Qi, J.; Fan, S. S. *Diam. Relat. Mater.* **2005**, *14*, 1695.
(39) Hafner, J. H.; Cheung, C. L.; Lieber, C. M. *Nature* **1999**, *398*, 761.

NL072298Y